Mesenchymal stromal cells mediate a switch to alternatively activated monocytes/macrophages after acute myocardial infarction

Victor Dayan · Gustavo Yannarelli ·
Filio Billia · Paola Filomeno · Xing-Hua Wang ·
John E. Davies · Armand Keating

Abstract Given the established anti-inflammatory properties of mesenchymal stromal cells (MSCs), we investigated their effect on inflammatory cell infiltration of ischemic cardiac tissue and cardiac function. We employed two types of MSCs, human bone marrow-derived (BM) MSCs and human umbilical cord perivascular cells in an experimental acute myocardial infarction (MI) model with the immune-deficient NOD/SCID gamma null mouse. Cells were infused 48 h after induction of MI and mice assessed 24 h later (72 h after MI) for bone marrow (BM), circulating and cardiac tissue-infiltrating monocytes/macrophages. We showed that in the presence of either MSC type, overall macrophage/monocyte levels were reduced, including pro-inflammatory M1-type macrophages, while the proportion of alternatively activated M2-type macrophages was significantly increased in the circulation and heart but not the BM. Moreover, we found decreased expression of IL-1β and IL-6, increased IL-10 expression and fewer apoptotic cardiomyocytes without changes in angiogenesis in the infarct area. Fractional shortening was enhanced 2 weeks after cell infusion but was similar to medium controls 16 weeks after MI. In vitro studies showed that BM MSCs increased the frequency of alternatively activated monocytes/macrophages, in part by MSC-mediated secretion of IL-10. Our data suggest a new mechanism for MSC-mediated enhancement of cardiac function, possibly via an IL-10 mediated switch from infiltration of pro-inflammatory to anti-inflammatory macrophages at the infarct site. Additional studies are warranted confirming the role of IL-10 and augmenting the anti-inflammatory effects of MSCs in cardiac regeneration.

V. Dayan · G. Yannarelli · P. Filomeno · X.-H. Wang ·
A. Keating
Cell Therapy Program, Princess Margaret Hospital,
University Health Network, University of Toronto,
Toronto, Canada

V. Dayan (✉)
26 de Marzo 3459/602, Montevideo, Uruguay
e-mail: victor_dayan@hotmail.com

F. Billia
Division of Cardiology,
Campbell Family Institute for Breast Cancer Research,
University Health Network, Toronto, Canada

J. E. Davies · A. Keating
Institute of Biomaterials and Biomedical Engineering,
University of Toronto, Toronto, Canada

Introduction

Mesenchymal stromal cells (MSCs) are increasingly investigated for the repair of injured tissue [32]. Administration of MSCs in animal models of myocardial infarction (MI) and ischemic cardiomyopathy yield variable degrees of functional improvement [1]. Current explanations favor paracrine mechanisms to account for enhanced function [32].

BM MSCs have cardiac protective properties that decrease with increasing donor age [10]. A new type of MSC with less donor variability and a more rapid doubling time, the human umbilical cord perivascular cell (HUCPVC) [28], may circumvent this limitation and given

its abundant availability, may be an alternative for cell therapy.

Monocytes/macrophages comprise two types, the classically activated and pro-inflammatory M1 type and alternatively activated M2 or anti-inflammatory cells [21]. After MI, initial infiltration occurs with monocytes/macrophages that express a predominant pro-inflammatory secretion profile (classically activated with high levels of IL-1β, IL-6 and TNFα) followed by anti-inflammatory monocytes/macrophages that are alternatively activated and secrete high levels of IL-10 [11, 23]. No single marker distinguishes the two cell types but differential expression of the surface markers, CD206 (an alternative activation marker) and Ly6C (a marker of classically activated cells) as well as gene expression of classically activated (IL-1β, IL-6) and alternatively activated (TGF-β, IL-10, CD163, Arginase-1) macrophages can help identify the subpopulations [4, 23, 26].

Human BM MSCs increase macrophage infiltration during wound healing presumably via a paracrine mechanism, as well as have a role in modulating their activation state but no study has addressed their role in regulating the subtype of monocytes/macrophages that infiltrate myocardium after MI, nor the mechanism(s) by which they exert the phenotype switch [6, 20]. We wished to test the hypothesis that MSCs mediate a switch in the circulating and infiltrating monocyte/macrophage phenotype after MI, thereby influencing short- and long-term functional outcomes.

We found that both BM MSCs and HUCPVCs, systemically infused 48 h after MI, increased alternatively activated monocytes/macrophages in the circulation as well as infiltrating cardiac tissue. These findings were associated with decreased pro-inflammatory and increased anti-inflammatory cytokines. MSC-treated animals exhibited functional improvement 2 and 4 weeks after MI as well as decreased cardiac remodeling and reduced pulmonary congestion 16 weeks after MI. We also showed in vitro that BM MSCs may influence the anti-inflammatory switch by secreting IL-10.

Materials and methods

Cell preparation

Human BM MSCs were obtained from healthy adult volunteers after informed consent according to a protocol approved by the University Health Network Research Ethics Board. Cells were cultured and passaged up to 4 times according to our established methods and characterized before infusion (see Supplemental Data).

HUCPVCs were obtained and passaged 4 times according to an established protocol and characterized before infusion (Figure S1).

Experimental acute MI model in immune-deficient mice

Procedures conformed to the Guide for the Care and Use of Laboratory Animals published by the US National Institute of Health. Female NOD-SCID IL2Rgamma(null) mice ($n = 42$) aged 10–12 weeks were used. A 7-0 silk suture (ETHICON) was passed underneath the left anterior descending coronary artery 1–3 mm from tip of the left auricle and ligation was performed. Ischemia was confirmed by myocardial blanching and ventricular arrhythmia (see Supplemental Data).

Infusion of BM MSCs and HUCPVCs

Forty-eight hours after MI, mice were randomly assigned to one of the following groups (14 per group): (1) Dulbecco minimum essential medium (DMEM) alone, (2) BM MSC 2×10^6 cells, and (3) HUCPVCs 2×10^6 cells. Cells were suspended in 200 μl of DMEM medium and infused via tail vein with a 28G needle. Successful i.v. infusion was monitored by lack of extravasation at the injection site.

Flow cytometric analysis

BM, blood and cardiac tissue obtained from mice killed ($n = 6$) were analyzed 72 h after MI for quantification of CD206, major histocompatibility complex type II (MHCII), CD62L and Ly6C monocytes/macrophages. Monocytes and macrophages were distinguished from other leukocytes by flow cytometry represented as low orthogonal (side) scatter and high levels of CD11b expression and are designated as CD11b+ cells [31] (see Supplemental Data and Figure S2).

Assay of leukocyte infiltration in heart tissue 72 h after MI

Frozen heart sections of 5 μm were stained with anti-mouse anti-Ly-6G and Ly-6C (BD Pharmingen, cat# 550291) (Gr-1) and F4/80 (Serotec, cat# MCA497GA) as described in Supplemental Data.

Real-time PCR assays for human Alu sequences

DNA was extracted from mouse heart, lung, spleen, liver, and bone marrow and subjected to real-time PCR for human Alu sequences (see Supplemental Data and Figure S3).

Real-time RT-PCR analysis for selected murine and human mRNAs

Quantitative RT-PCR was performed using mouse-specific primers for the quantification of IL-1β, IL-6, IL-10, TNFα, TGF-β, Bax, Bcl2, VEGF, CX3CL1, CCL2, E-selectin, ICAM, VCAM, Arginase-1 and CD163 on infarcted cardiac tissue and in vitro bone marrow-derived macrophages after co-culture (Table S1). Human-specific primers were constructed (Fwd: GGCGCTGTCATCGATTTCTT; Rev: TTGGAGCTTATTAAAGGCATTCTTC) for quantification of IL-10 expression in BM MSCs after co-culture with mouse macrophages.

In situ end-labeling (ISEL) for apoptosis

Heart sections from mice killed 72 h after MI were stained for apoptotic cardiomyocytes defined by nuclear morphology. The ISEL technique was used as described in Supplemental data.

Echocardiography

Transthoracic echocardiographic imaging was performed by a blinded observer using a dedicated Vivid7 (15 MHz linear epicardial surgical probe, General Electric) machine. The following measurements were obtained at baseline (before MI induction), 2, 4 and 16 weeks: fractional shortening (FS), left ventricular end-systolic and diastolic diameter and septum thickness (see Supplemental Data).

Microscopic examination of the myocardium

At 16 weeks after MI, heart and lungs were harvested and weighed. Tissue was stained with Masson's trichrome to measure scar area, thickness and septum width and with CD31 immunostaining for vessel quantification. (see Supplemental data for details).

In vitro co-culture of BM-derived macrophages and BM MSCs

BM-derived macrophages were obtained as previously described [18]. BM was extracted from 10- to 12-week old NOD/SCID gamma null female mice. After centrifugation, cells were suspended in RPMI 1640 medium supplemented with 10% FBS, 1% penicillin/streptomycin and 25 μg/ml M-CSF and plated in 6-well plates at 2×10^6 cells/ml for 24 h and non-adherent cells were collected, counted and plated at the concentration above. After 3 days, medium was removed and plates were divided into 5 groups (3 per group): (1) control (DMEM), (2) human BM MSCs in DMEM (2×10^5 cells/ml), (3) human BM MSCs conditioned medium obtained after 24 h of totally confluent BM MSCs, (4) same as (3) but with anti-human IL-10 (10 μg/ml) and (5) human recombinant IL-10 (100 U/ml) (eBioscience) as previously described [7, 19, 20]. Specificity of anti-human IL-10 was confirmed by dot blot assay (Figure S4). In each case, fresh RPMI 1640 was added in a 1:1 ratio.

Proliferation of macrophages was assessed using PKH-26 (Sigma) (2 μM) (for CD206 macrophages) and CFSE (for Ly6C macrophages) staining [3, 13]. Different stains (PKH-26 and CFSE) were used to avoid overlap of fluorescence (anti-CD206 was FITC conjugated and anti-Ly6C, PE conjugated). For PKH-26 staining, macrophages were cultured initially for 3 days. Medium was removed and PKH-26 added at RT for 2–5 min. Inactivation was done using FBS for 1 minute. BM MSCs or BM MSC-conditioned medium was added after extensive PBS wash of stained macrophages. Macrophages were stained with CFSE (Molecular Probes, Eugene, Oregon, USA) prior to plating [16]. Cells were suspended in 1 ml of PBS and 1 μl of prepared CFSE solution (2.5 μM) and incubated at 37°C for 5 min with gentle agitation. The labeling reaction was stopped by adding 1 ml of heat-inactivated FBS. Cells were washed in PBS and plated as described. After 3 days of culture, BM MSCs or BM MSC conditioned medium was added.

Flow cytometric analysis of experimental groups was performed after 3 days of co-culture. Detached cells were co-stained with APC conjugated anti- mouse CD11b and FITC conjugated CD206 or PE conjugated Ly6C. Apoptosis of Ly6Chi macrophages was determined after co-culture by co-staining with APC-CD11b, PE-Ly6C and FITC conjugated anti-Annexin V. Dead cells were excluded from analysis using propidium iodide (PI). At least 20,000 events were used for analysis.

Statistical analysis

Quantitative data are expressed as mean ± SEM. Statistical analysis was performed by one-way ANOVA, followed by the Bonferroni test for comparisons between groups at specific time-points in vivo (72 h or 16 weeks from MI) and in vitro. Two-way ANOVA, followed by Bonferroni multiple comparisons, was used to compare groups at different time-points (fractional shortening, left ventricular dimensions, septum thickness). Survival was analyzed using the Kaplan–Meyer product limit estimate and compared with the log-rank test. A value of $p < 0.05$ was considered statistically significant.

Results

BM MSCs and HUCPVCs promote a switch to alternatively activated circulating and infiltrating monocytes/macrophages after MI

Experimental MI was generated in NOD/SCID gamma null mice. BM MSCs, HUCPVCs or medium were infused intravenously 48 h later. Total number of monocyte/macrophage (CD11b + cells) cells in cardiac tissue was lower in BM MSC (390 ± 58 cells, $p < 0,05$) and HUCPVC groups (564 ± 87 cells, p = ns) than in medium treated mice (1,134 ± 238 cells) (Fig. 1a). Leukocyte infiltration in the infarcted myocardial tissue (Ly6G/Ly6C cells) was significantly lower for BM MSC (584 ± 92 cells/mm^2, $p < 0.01$) and HUCPVC (545 ± 59 cells/mm^2, $p < 0.01$) mice compared with medium controls (1,460 ± 238 cells/mm^2) (Fig. 1b). Macrophage (F4/80 + cells) infiltration in infarcted tissue was significantly higher in the BM MSC (608 + 108 cells/mm^2, $p < 0.01$) and HUCPVC (538 + 65 cells/mm^2, $p < 0.01$) groups compared with medium controls (29 + 4 cells/mm^2) (Fig. 1c). Quantification and the immunophenotype of monocytes/macrophages (as % of total cells) 24 h after infusion showed that BM macrophages (31.2 + 1.7 vs. 38.5 + 1.8%, $p < 0.05$), circulating monocytes (7.3 + 0.9 vs. 36.6 + 0.6%, $p < 0.001$) and cardiac infiltrating monocytes/macrophages (0.57 + 0.06 vs. 1.65 + 0.65%, $p < 0.05$) were decreased in the BM MSC group compared with medium controls, respectively (Fig. 1h, f and d). Infusion of HUCPVCs decreased BM macrophages (31.2 + 1.8%, $p < 0.05$) and circulating monocytes (27 + 1.6%, $p < 0.001$) compared with medium-injected mice.

A higher percentage of CD206+ monocytes/macrophages was detected infiltrating the hearts of mice infused with BM MSCs (77.2 + 2.2%, $p < 0.05$) and HUCPVCs (81.3 + 2%, $p < 0.05$) compared with medium controls (50 + 8%) (Fig. 1e) The percentage of circulating CD206+ monocytes was significantly higher in the BM MSC (21.5 + 1.3%, $p < 0.01$) and HUCPVC (15.7 + 1.2%, $p < 0.05$) groups compared with medium-injected mice (4.9 + 2.5%) (Fig. 1g). No difference in the percentage of CD206+ macrophages was noted in the BM (Fig. 1i).

Representative microphotographs of leukocytes and macrophages in cardiac tissue are shown in Fig. 2.

No differences were found in the frequency of Ly6Chi or MHCII-expressing macrophages among groups in BM, blood or heart (Figure S5, A and B). CD62L-expressing monocytes/macrophages were similar between groups at each site (Figure S5, C).

Quantification of cytokine expression by PCR in infarcted tissue showed that BM MSC and HUCPVC-injected mice had lower expression of IL-1β (3.90 + 0.75-fold,

$p < 0.001$ and 6.67 + 1.04-fold, $p < 0.01$) versus controls (15.05 + 1.85-fold); IL-6 expression was also decreased in BM MSC (82.04 + 12.90-fold, $p < 0.001$) and HUCPVC-treated animals (88.91 + 13.25-fold, $p < 0.001$) compared with medium-injected mice (220.70 + 7.66-fold). Higher expression of IL-10 in mice treated with BM MSCs (9.59 + 0.66-fold, $p < 0.001$) and HUCPVCs (6.52 + 0.80-fold, $p < 0.05$) was found compared with medium controls (2.79 + 0.22). There were no differences in TNF-α, TGF-β and VEGF expression among groups (Fig. 3).

Cardiac expression of vascular adhesion molecules (VCAM, ICAM and E-Selectin) and chemokines (CX3CL1 and CCL2) was similar among groups (Figure S6).

BM MSCs and HUCPVCs decrease frequency of apoptotic cells after MI

The frequency of apoptotic cardiomyocytes in the MI area evaluated by ISEL was decreased in mice injected with BM MSCs (49 + 13 cells/mm^2, $p < 0.001$) and HUCPVCs (58 + 6 cells/mm^2, $p < 0.001$) compared with medium (152 + 21 cells/mm^2) (Fig. 4a).

Histological determination of apoptosis was confirmed by molecular assessment of Bax/Bcl2 (an index of whole tissue cell apoptosis) using PCR in the MI area. The apoptotic index was lower in the BM MSC (1.27 + 0.21-fold, $p < 0.001$) and HUCPVC (1.88 + 0.25-fold, $p < 0.01$) groups compared with control mice (3.44 + 0.39-fold) (Fig. 4b).

Injected cells localize mainly to the lung

Real-time PCR of human Alu sequences, showed that 24 h after cell injection, most cells were trapped in the lung, as previously described [14] (Fig. 5). A higher amount of human DNA was found in the HUCPVC-injected group compared with BM MSC-treated animals. In both cases, the amount of human DNA in infarcted and non-infarcted tissue was very small (from 0.0002 to 0.001% of total DNA). Human DNA was not detectable in cell-treated mouse BM or in medium-treated animals.

### BM MSCs and HUCPVCs improve short-term cardiac function and decrease long-term cardiac remodeling

Two weeks after MI, LV fractional shortening (FS) was significantly better in mice receiving BM MSCs (43.3 + 0.6%, $p < 0.001$) and HUCPVCs (39.8 + 0.8%, $p < 0.01$) compared with medium (34.4 + 1.3%). At 4 weeks, FS was better in BM MSC and HUCPVC-treated mice versus control animals ($p < 0.05$) but at 16 weeks after infusion cell-treated and medium groups had similar values (Fig. 6a).

Fig. 1 BM MSCs and HUCPVCs modulate the frequency of circulating and cardiac infiltrating monocytes/ macrophages after 72 h of experimental MI. a Total monocyte/macrophage, b leukocyte and c macrophage frequency in cardiac tissue. d Monocyte/Macrophage and e CD206+ cells as % of total and CD11b cells, respectively, in cardiac tissue. f Monocyte and g CD206+ cells frequency in blood expressed as % of total and CD11b cells, respectively. h Monocyte/Macrophage and i CD206+ cells frequency in BM expressed as % of total and CD11b cells, respectively. Data represent mean + SEM; $n = 6$ mice per group. $*p < 0.05$, $**p < 0.01$ and $***p < 0.001$ versus medium. $^{†††}p < 0.001$ versus HUCPVC
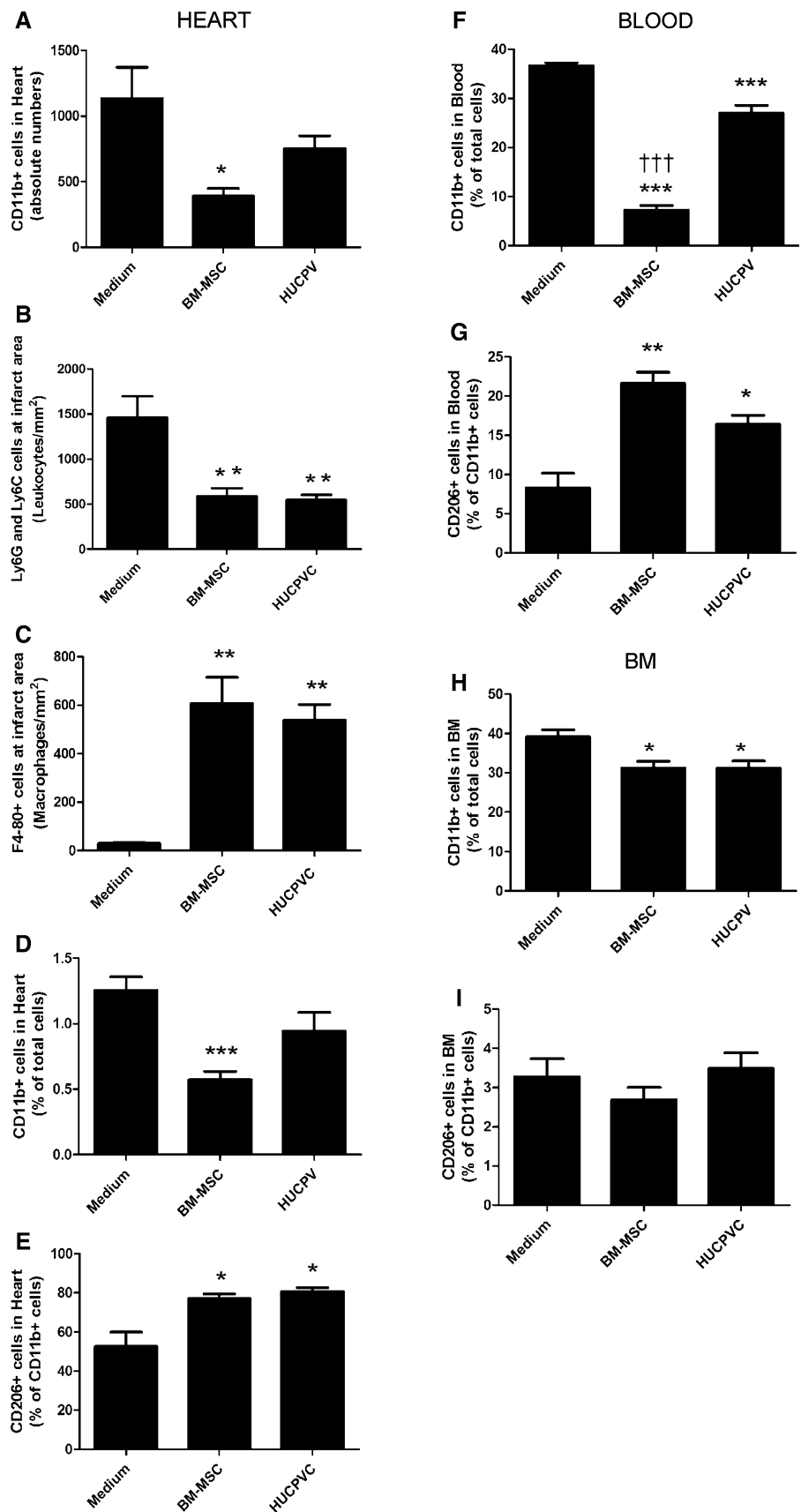
Fig. 2 Inflammatory cell infiltration at infarct area evaluated by immunohistochemistry after 72 h of MI. **a** Microphotograph of representative Ly6C and Ly6C staining. **b** Representative microphotograph of ISEL staining. *Scale bar* 100 μm
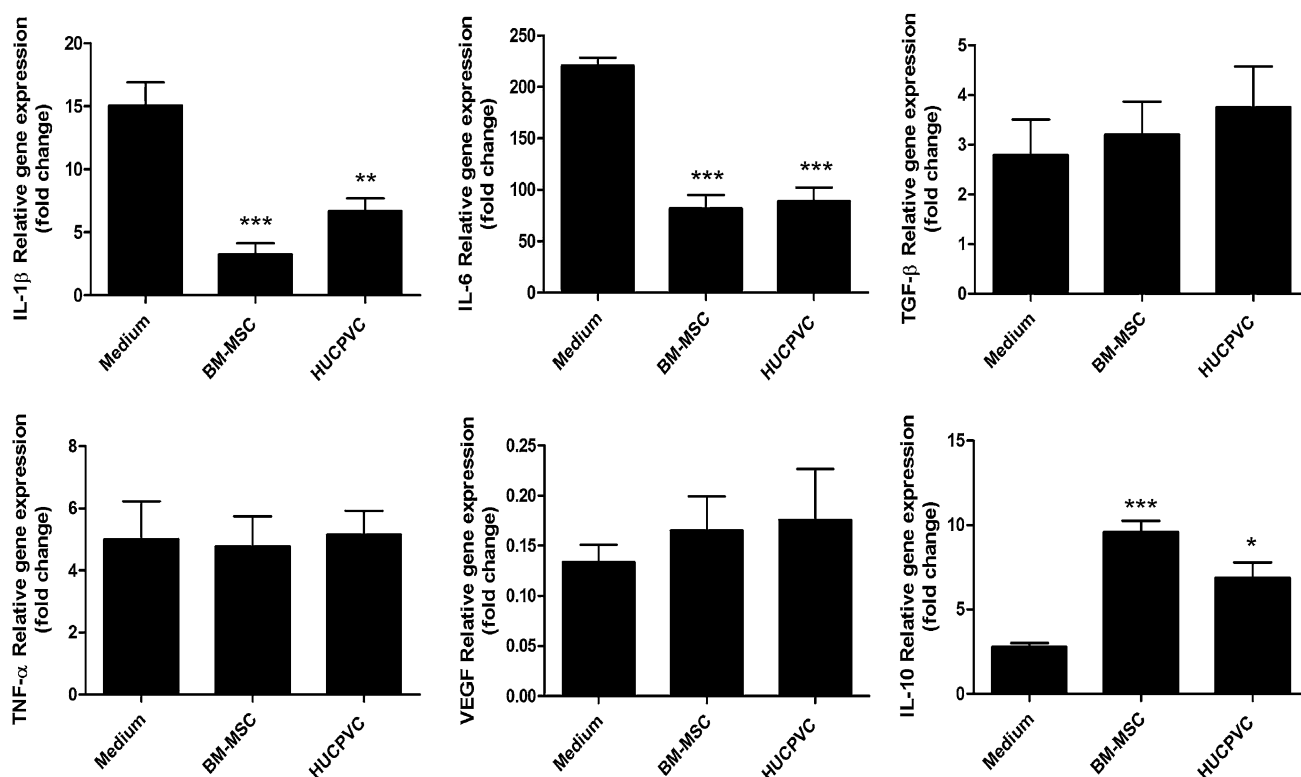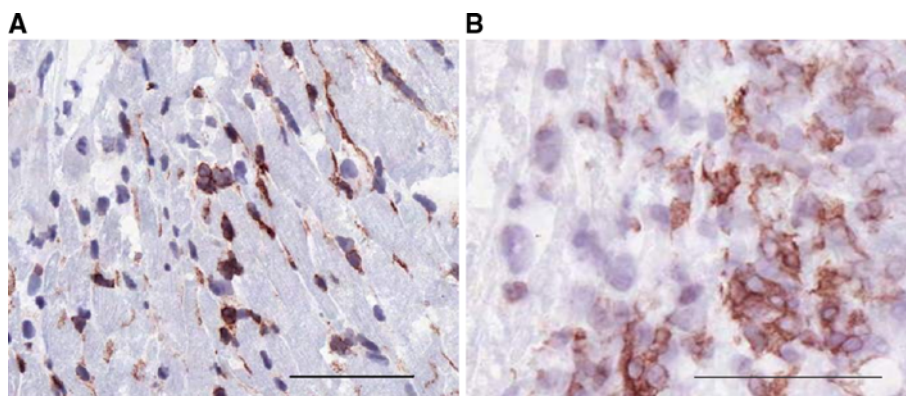
Fig. 3 Real-time RT-PCR of mRNA from the infarcted area (taken after 72 h of MI) normalized to age-matched non-infarcted NOD/SCID gamma null mice. Gene expression was quantified from myocardial tissue. Normalized data are expressed as mean ± SEM; $n = 6$ per group. $*p < 0.05$, $**p < 0.01$ and $***p < 0.001$ versus medium

LVEDD and LVESD were not different among the groups at all evaluated time-points (Fig. 6b, c). Nonetheless, BM MSCs or HUCPVCs decreased septum thickness compared with medium ($p < 0.05$) 16 weeks after MI (Fig. 6d). Myocardial scar area or scar thickness was similar among groups (Fig. 6e–i). Septum thickness, however, was significantly greater in the medium-treated mice ($1.8 + 0.1$ mm, $p < 0.05$) than in cell-treated groups (Fig. 6j) at postmortem. Vessel quantification in the scar and peri-scar areas showed no differences among groups 16 weeks after MI (Fig. 6k–l).

Total weight of mice in all groups was similar at the 16-week end-point and no difference was detected in LV/total body weight index among groups (Fig. 7a, b). Pulmonary congestion measured as lung/total body weight index was lower in BM MSC ($0.0037 + 3.6 \times 10^{-5}$, $p < 0.01$) and HUCPVC ($0.0042 + 8.8 \times 10^{-5}$, $p < 0.05$) cohorts compared with medium-treated mice ($0.0052 + 20 \times 10^{-5}$) (Fig. 7c) [22].

No significant differences in the survival were found among groups during the follow-up period (Log-rank test, $p = 0.48$) (Fig. 7d).

Fig. 4 Evaluation of apoptosis by immunohistochemistry and real-time PCR of infarcted cardiac tissue after 72 h of MI. **a** Quantification of positive cells stained by ISEL technique from infarcted cardiac tissue. **b** Real-Time RT-PCR for Bax/Bcl2 of mouse mRNA from infarcted cardiac tissue. Values are normalized to age-matched non-infarcted NOD/SCID gamma null mice. Cell count expressed/mm^2 of tissue expressed as mean ± SEM; $n = 6$ per group. $**p < 0.01$ and $***p < 0.001$ versus medium. **c** Representative immunohistochemistry photomicrograph of infarcted area stained by ISEL. *Red-brownish* nuclei are positive. *Arrowhead* apoptotic cardiomyocyte. *Scale bar* 100 µm
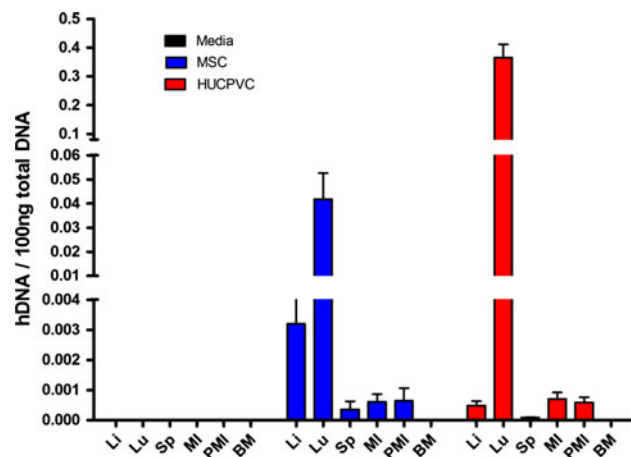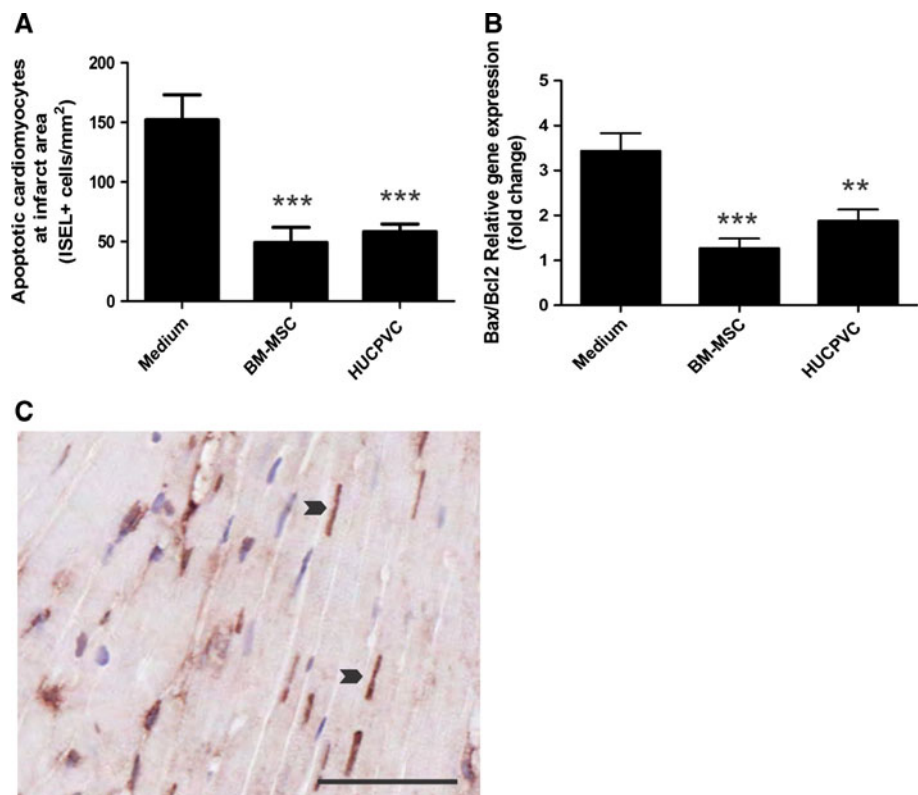
Fig. 5 Lodgement of human cells 24 h after infusion (72 h after MI). Real-time RT-PCR for human-specific Alu sequences. *Values* represent amount of human DNA (ng) in 100 ng of total DNA per organ sample. Data are expressed as mean ± SEM; $n = 6$ per group. *Li* liver, *Lu* lung, *MI* myocardial infarction, *PMI* peri-myocardial infarction, *Sp* spleen, *BM* bone marrow. $n = 8$ per group

Human BM MSCs switch BM-derived macrophages to an alternatively activated phenotype by secretion of IL-10

Mouse BM-derived macrophages were co-cultured with human BM MSCs or MSC-conditioned medium to evaluate the direct effect of MSCs on the macrophage phenotype and

to complement the in vivo data. The frequency of Ly6C + macrophages decreased after 3 days of co-culture with BM MSCs (0.81 + 0.06%, $p < 0.01$) or MSC-conditioned medium (1.01 + 0.07%, $p < 0.05$) compared with controls (1.70 + 0.20%). CD206− and MHCII-expressing macrophages increased after co-culture with BM MSCs (72.1 + 1 and 50.7 + 1.6%, $p < 0.001$ in both cases) or with BM MSC-conditioned medium (61.1 + 1.2 and 29.6 + 2.3%, $p < 0.001$ and $p < 0.01$, respectively) compared with controls (9.6 + 1.5 and 17.0 + 4.1%) (Fig. 8a–c).

While no differences in the frequency of apoptotic Ly6C + macrophages were observed between groups (Fig. 8d), proliferation (by CFSE fluorescence) was slightly decreased in co-cultures of BM MSCs ($p < 0.05$) (Fig. 8e). Proliferation of CD206+ macrophages was significantly higher ($\cong 35\%$) after co-culture with BM MSCs ($p < 0.001$) or BM MSC-conditioned medium ($p < 0.001$) (as determined by lower PKH-26 fluorescence) (Fig. 8f).

Gene expression of CD163 ($p < 0.01$), TGF-β ($p < 0.05$) and arginase-1 ($p < 0.05$) was significantly higher in macrophages co-cultured with BM MSCs than in the control group (Fig. 8g–i). IL-10 expression in co-cultured and conditioned medium-cultured macrophages was higher than in controls ($p < 0.001$) (Fig. 8j).

We next cultured BM-derived macrophages with BM MSC-conditioned medium and an anti-human IL-10 antibody and detected a twofold decrease in the up-regulation of CD206+ macrophages induced by BM MSC-conditioned
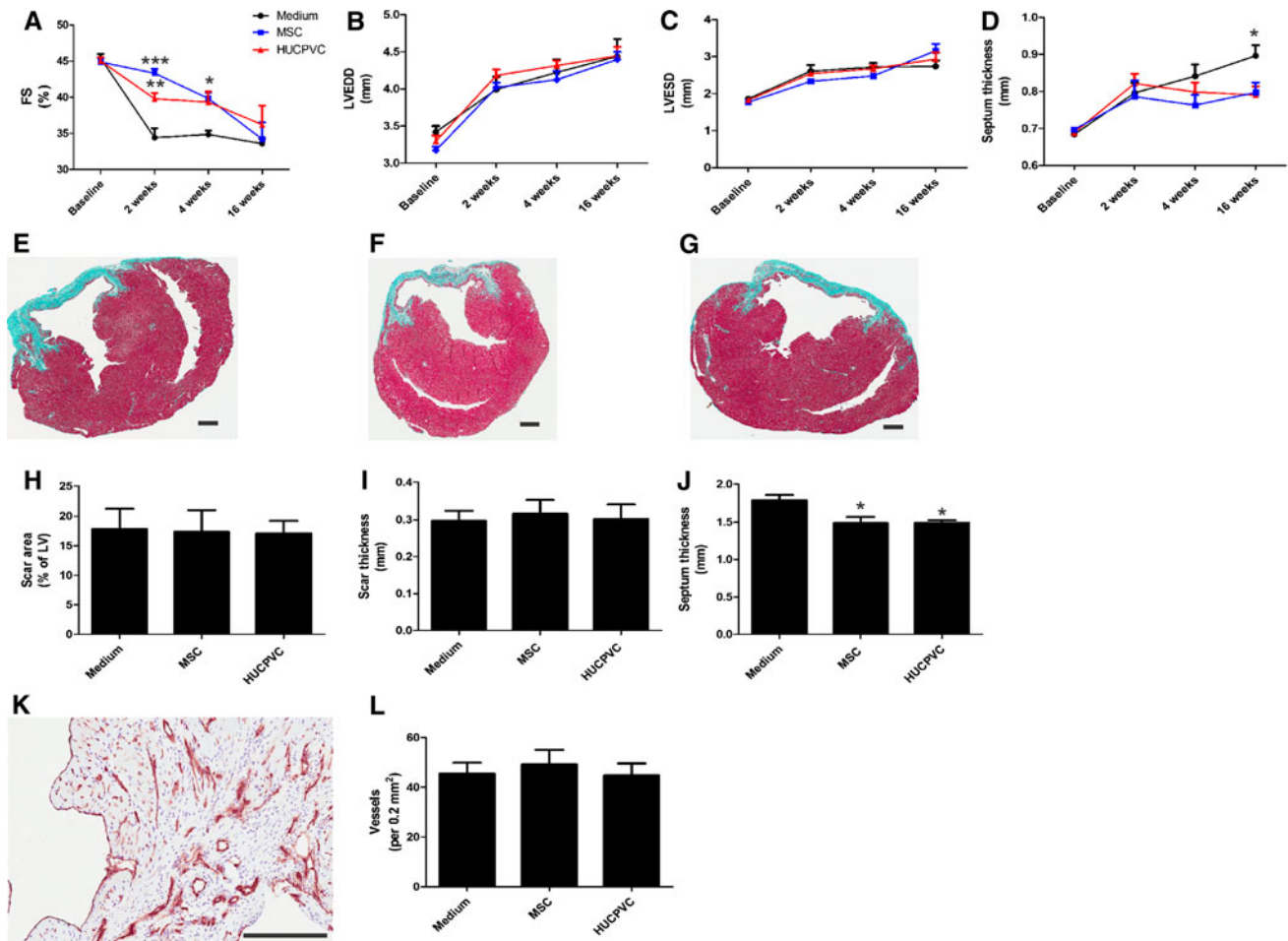
Fig. 6 Functional and histological outcomes after MI. **a** Fractional shortening (FS), **b** left ventricular end-diastolic diameter (LVEDD), **c** left ventricular end-systolic diameter (LVESD), **d** septum thickness measured at the baseline, 2, 4 and 16 weeks after MI. Representative Masson trichrome stains of heart tissue micrographs in animals 16 weeks after MI injected with **e** medium, **f** BM MSCs and **g** HUCPVC MI. Scar tissue stained in blue. **h** Scar area quantified as per cent of total LV area. **i** Scar and **j** septum thickness expressed in mm. **k** Representative cardiac immunohistochemical staining for CD31 16 weeks after MI. **l** Number of vessels/0.2 mm^2 of infarcted and peri-infarcted tissue. Data represent the mean ± SEM; $n = 6$–8.*$p < 0.05$; **$p < 0.01$ and ***$p < 0.001$ versus medium. *Scale bar* represents 100 μm

medium ($p < 0.01$) (Fig. 8k). Human recombinant IL-10 alone increased the frequency of CD206+ macrophages eightfold. Moreover, IL-10 expression in human MSCs increased almost threefold after co-culture with mouse macrophages (Fig. 8l).

Discussion

We have demonstrated for the first time that systemically infused human BM MSCs and HUCPVCs increase the frequency of alternatively activated anti-inflammatory monocytes/macrophages infiltrating injured myocardium after acute MI. The presence of increased circulating alternatively activated monocytes and an unaltered expression of chemokines and vascular adhesion molecules in infarct tissue suggest that the increase in alternatively activated macrophages infiltrating the heart may be due to a phenotype switch in circulating monocytes. Furthermore, our in vitro data suggest that the enhanced proportion of alternatively activated macrophages is in part related to the MSC-mediated secretion of IL-10.

In our experiments, mice treated with either type of MSC showed decreased systemic and BM monocytosis. Absence of human DNA in the marrow of recipient mice infers a paracrine mechanism of monocyte/macrophage suppression. We also found that MSCs increased the proportion of CD206+ and MHCII+ circulating monocytes. Given that no differences were detected in the ratio of monocyte/macrophage subtypes in the marrow, we presume the switch occurred either in the circulation and/or the spleen, although the latter was not tested. An increase

Fig. 7 Mice weight and survival 16 weeks after MI. **a** Total body weight, **b** left ventricular (LV)/total body weight, **c** lung weight/total body weight, comparison among groups at end-point. Values expressed in grams. **d** Survival curve. * and **$p < 0.05$ and $p < 0.01$, respectively
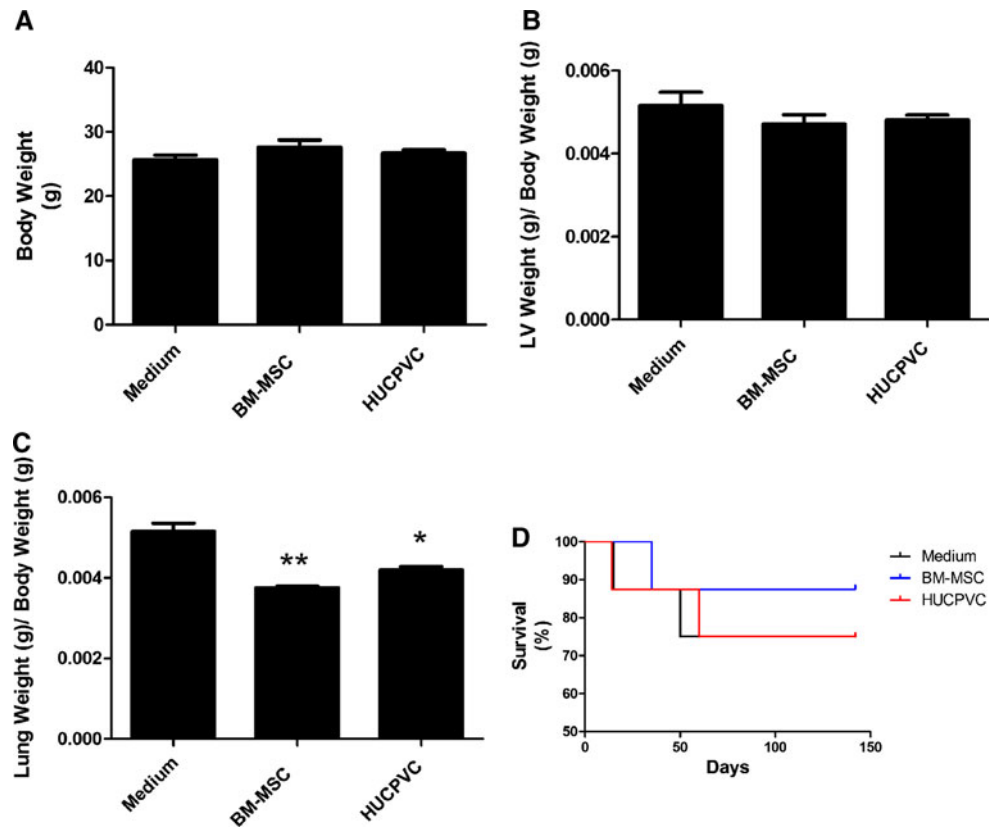
in M2 monocytes/macrophages was also evident among the cells infiltrating the injured myocardium. We propose the increase to be due to a higher proportion of circulating monocytes in the absence of changes in the expression of cardiac chemokines, vascular adhesion factors or monocyte/macrophage endothelial adhesion receptors (CD62L) in the injured myocardium. Both types of MSCs decreased the total number of infiltrating leukocytes (Ly6G and Ly6C) while increasing the mature F4-80+ macrophages which have been shown to be associated with an anti-inflammatory response and regenerative action [2, 15]. Reduced absolute numbers of infiltrating monocytes/macrophages as well as an increased proportion of CD206+ macrophages may also explain the decreased cardiac expression of IL-1β, IL-6, higher levels of IL-10, as well as the reduced frequency of apoptotic cardiomyocytes in MSC-treated mice [8, 30]. Our findings are supported by a recent study from Hu et al. [8] in which mice deficient for scavenger receptor A (homologous to the CD206 receptor) have a worse functional outcome as well as higher levels of M1 macrophage infiltration and IL-1, IL-6 secretion after AMI compared with wild type. This effect could be reversed after the transplantation of bone marrow from wild-type mice [8].

Our data showing an improvement in cardiac function in MSC-treated mice may therefore be explained, in part, by a reduction in the negative inotropes, IL-1 and IL-6, and an increase in IL-10, known to have a positive inotropic effect [9, 12, 25]. It has also been shown that cytokines can induce cardiac stem cells to proliferate and have a role in Wnt signaling under ischemic conditions and may therefore also contribute to the functional improvement [17, 24]. Nevertheless, definitive answers to address the observed improvements remain unclear.

The infusion of BM MSCs and HUCPVCs was associated with improved cardiac function 2 and 4 weeks after MI as well as decreased cardiac remodeling (reduced septal wall thickness) and reduced pulmonary congestion at 16 weeks. In preliminary experiments, we further delineated the role of macrophages in MSC-mediated cardiac improvement after MI. We treated mice with liposomal clodronate in an attempt to remove the cells from the circulation prior to MI and MSC infusion [20]. All mice died within 24 h of clodronate infusion (data not shown). While clodronate can successfully remove macrophages in immunocompetent mice, experiments with this agent in our highly immuno-deficient NOD/SCID gamma null mouse model were not feasible and were not part of our methodology [23].

We also evaluated the role of neo-angiogenesis as a possible explanation for the improvement in cardiac function but found no differences in VEGF gene expression levels or vessel density among the groups at early or late end-points, respectively, as was previously shown [29].
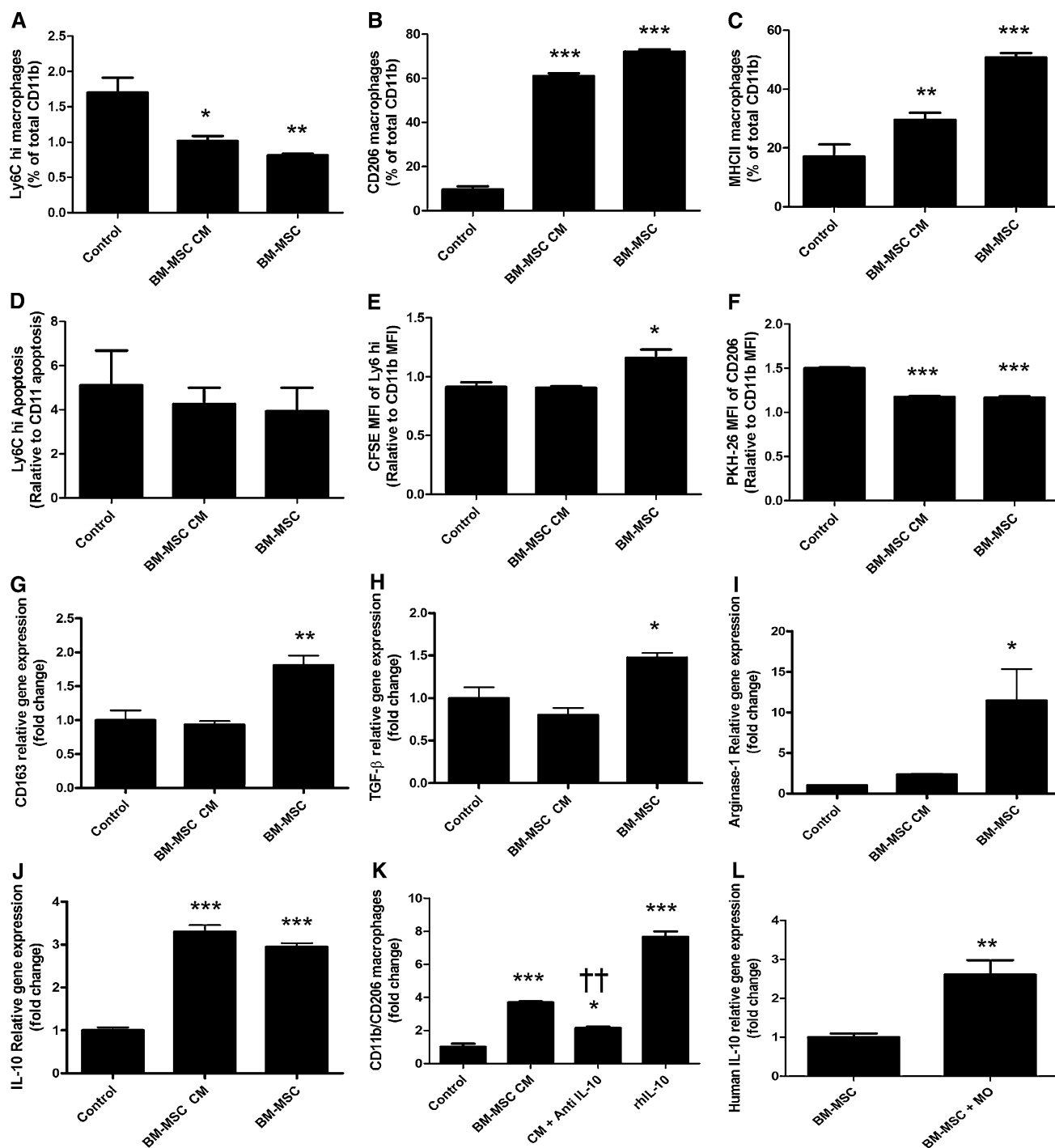
Fig. 8 Characterization of mouse BM-derived macrophages after 3 days co-culture with human BM MSCs or BM MSC-conditioned medium. Flow cytometric analysis of **a** Ly6Chi+ cells, **b** CD206+ cells and **c** MHC II+ cells. Values are expressed as percent of live macrophages. **d** Ly6Chi macrophage apoptosis after co-culture relative to apoptosis of CD11b+ cells, **e** CFSE mean fluorescence intensity (MFI) of Ly6Chi cells, **f** PKH-26 MFI of CD206+ macrophages. Values are relative to PKH-26 and CFSE MFI of total macrophage population. Quantification of **g** CD163+ cells, **h** TGF-β, **i** Arginase-1 and **j** IL-10 mouse specific mRNA expression after co-culture. **k** Flow cytometric quantification of CD206+ macrophages after 3 days culture with BM MSC-conditioned medium with or without anti-human IL-10 and macrophages with human recombinant IL-10 (rhIL-10); **l**) Human BM MSC IL-10 human-specific mRNA expression after co-culture. Values are normalized to the control group. All data are expressed as mean ± SEM; $n = 3$ per group. *$p < 0.05$; **$p < 0.01$ and ***$p < 0.001$ versus control. ††$p < 0.01$ versus BM MSC CM

IL-10 is a negative immune regulator involved in the differentiation of naive T cells into regulatory T cells with immunosuppressive and anti-inflammatory actions. In mice after MI, IL-10 reduces macrophage infiltration, myocardial pro-inflammatory cytokine expression and improves cardiac function [12]. The hemodynamic improvement after direct injection of BM mononuclear cells in an acute cardiac ischemia mouse model is related to decreased T cell accumulation and is not reproduced with IL-10 knockout cells [5]. Rat MSCs retrovirally transduced to express IL-10 improved lung ischemia–reperfusion injury and reduced apoptotic cells as well as infiltrating T cells [20, 33]. Other hematopoietic cytokines such as GM-CSG have also shown to regulate cardiac repair [27].

We found that BM MSCs or BM MSC-conditioned medium increased the proportion of CD206+ cells consistent with our in vivo results. After co-culture with BM MSCs, the absolute number of CD206+ BM-derived macrophages increased, inferring proliferation of a CD206+ precursor population. We obtained similar results with BM MSC-conditioned medium suggesting a paracrine effect. In addition, BM MSCs or their conditioned medium decreased levels of classically activated Ly6C+ macrophages attributable at least partially to inhibition of proliferation.

We further investigated the role of MSCs in increasing the level of CD206+ macrophages. We confirmed that human BM MSCs upregulate IL-10 expression when co-cultured with mouse macrophages. We next tested the effect of a specific human IL-10 blocking antibody in cultures of mouse BM macrophages and human BM MSC-conditioned medium and found a twofold decrease in the frequency of CD206+ cells compared with cultures in the absence of the antibody. The specificity of the antibody was confirmed in experiments showing lack of cross-reactivity with mouse IL-10 (Figure S4). These in vitro data provide preliminary additional evidence for MSC-mediated IL-10 release underlying the increase in alternatively activated macrophages.

Our data show that BM MSCs and HUCPVCs exert a similar effect on cardiac function after intravenous infusion, although some differences were observed. For example, higher levels of human DNA were detected in the lungs of HUCPVC versus BM MSC-treated mice, possibly the result of differences in adhesion molecule expression and the larger size of HUCPVCs, favoring greater entrapment in the pulmonary vasculature.

Infusion of either BM MSCs or HUCPVCs reduced the infiltration of leukocytes and the expression of IL-1β and increased IL-10 expression in the MI area. These changes were greater in the BM MSC-treated mice and may explain the lower level of apoptotic cardiomyocytes and superior cardiac function at the same dose 2 weeks after MI.

We recognize several limitations of our model. The first is inherent to in vivo study of human MSCs in a xenogeneic model. We chose the highly immune-deficient NOD SCID gamma null mouse model which lacks B, T and NK cells, hence cannot assess the effects on much of the recipient immune system. The second is that we have only in vitro data implicating the role of MSC-mediated IL-10 in driving the switch to M2 macrophages. A definite answer to this dilemma would be to reproduce these experiments using IL-10 gene-silenced human MSCs and evaluate macrophage infiltration.

In summary, we have shown that after MI, BM MSCs and HUCPVCs mediate a switch of monocytes/macrophages to an anti-inflammatory activation state that may be associated with enhanced cardiac function. Our in vitro studies showed that BM MSCs activated alternative macrophages by secretion of IL-10. Our results provide new evidence for a novel mechanism of action of human BM MSCs and suggest that additional studies are warranted to further investigate the role of IL-10 secretion by MSCs in cardiac regeneration after MI.

References

1. Amado LC, Saliaris AP, Schuleri KH, St John M, Xie JS, Cattaneo S, Durand DJ, Fitton T, Kuang JQ, Stewart G, Lehrke S, Baumgartner WW, Martin BJ, Heldman AW, Hare JM (2005) Cardiac repair with intramyocardial injection of allogeneic mesenchymal stem cells after myocardial infarction. Proc Natl Acad Sci USA 102:11474–11479. doi:10.1073/pnas.0504388102
2. Arnold L, Henry A, Poron F, Baba-Amer Y, van Rooijen N, Plonquet A, Gherardi RK, Chazaud B (2007) Inflammatory monocytes recruited after skeletal muscle injury switch into antiinflammatory macrophages to support myogenesis. J Exp Med 204:1057–1069. doi:10.1084/jem.20070075
3. Bennett S, Por SB, Cooley MA, Breit SN (1993) In vitro replication dynamics of human culture-derived macrophages in a long term serum-free system. J Immunol 150:2364–2371
4. Bréchot N, Gomez E, Bignon M, Khallou-Laschet J, Dussiot M, Cazes A, Alanio-Bréchot C, Durand M, Philippe J, Silvestre JS, Van Rooijen N, Corvol P, Nicoletti A, Chazaud B, Germain S (2008) Modulation of macrophage activation state protects tissue from necrosis during critical limb ischemia in thrombospondin-1-deficient mice. PLoS One 3:e3950. doi:10.1371/journal.pone.0003950
5. Burchfield JS, Iwasaki M, Koyanagi M, Urbich C, Rosenthal N, Zeiher AM, Dimmeler S (2008) Interleukin-10 from transplanted bone marrow mononuclear cells contributes to cardiac protection after myocardial infarction. Circ Res 103:203–211. doi:10.1161/CIRCRESAHA.108.178475

6. Chen L, Tredget EE, Wu PY, Wu Y (2008) Paracrine factors of mesenchymal stem cells recruit macrophages and endothelial lineage cells and enhance wound healing. PLoS One 3:e1886. doi:10.1371/journal.pone.0001886

7. Elenkov IJ, Webster E, Papanicolaou DA, Fleisher TA, Chrousos GP, Wilder RL (1998) Histamine potently suppresses human IL-12 and stimulates IL-10 production via H2 receptors. J Immunol 161:2586–2593

8. Hu Y, Zhang H, Lu Y, Bai H, Xu Y, Zhu X, Zhou R, Ben J, Xu Y, Chen Q (2011) Class A scavenger receptor attenuates myocardial infarction-induced cardiomyocyte necrosis through suppressing M1 macrophage subset polarization. Basic Res Cardiol. doi:10.1007/s00395-011-0204-x

9. Jackson KA, Majka SM, Wang H, Pocius J, Hartley CJ, Majesky MW, Entman ML, Michael LH, Hirschi KK, Goodell MA (2001) Regeneration of ischemic cardiac muscle and vascular endothelium by adult stem cells. J Clin Invest 107:1395–1402. doi:10.1172/JCI12150

10. Khan M, Mohsin S, Khan SN, Riazuddin S (2011) Repair of senescent myocardium by mesenchymal stem cells is dependent on the age of donor mice. J Cell Mol Med 15:1515–1520. doi:10.1111/j.1582-4934.2009.00998

11. Kleinbongard P, Heusch G, Schulz R (2010) TNFalpha in atherosclerosis, myocardial ischemia/reperfusion and heart failure. Pharmacol Ther 127:295–314. doi:10.1016/j.pharmthera.2010.05.002

12. Krishnamurthy P, Rajasingh J, Lambers E, Qin G, Losordo DW, Kishore R (2009) IL-10 inhibits inflammation and attenuates left ventricular remodeling after myocardial infarction via activation of STAT3 and suppression of HuR. Circ Res 104:e9–e18. doi:10.1161/CIRCRESAHA.108.188243

13. Lee GM, Fong S, Francis K, Oh DJ, Palsson BO (2000) In situ labeling of adherent cells with PKH26. In Vitro Cell Dev Biol Anim 36:4–6. doi:10.1290/1071-2690

14. Lee RH, Pulin AA, Seo MJ, Kota DJ, Ylostalo J, Larson BL, Semprun-Prieto L, Delafontaine P, Prockop DJ (2009) Intravenous hMSCs improve myocardial infarction in mice because cells embolized in lung are activated to secrete the anti-inflammatory protein TSG-6. Cell Stem Cell 5:54–63. doi:10.1016/j.stem.2009.05.003

15. Lichtenauer M, Mildner M, Baumgartner A, Hasun M, Werba G, Beer L, Altmann P, Roth G, Gyöngyösi M, Podesser BK, Ankersmit HJ (2011) Intravenous intramyocardial injection of apoptotic white blood cell suspensions prevents ventricular remodelling by increasing elastin expression in cardiac scar tissue after myocardial infarction. Basic Res Cardiol 106:645–655. doi:10.1007/s00395-011-0173-0

16. Lyons AB (2000) Analysing cell division in vivo, in vitro using flow cytometric measurement of CFSE dye dilution. J Immunol Methods 243:147–154. doi:10.1016/S0022-1759(00)00231-3

17. Madonna R, Rokosh G, De Caterina R, Bolli R (2010) Hepatocyte growth factor/Met gene transfer in cardiac stem cells–potential for cardiac repair. Basic Res Cardiol 105:443–452. doi:10.1007/s00395-010-0102-7

18. Maggini J, Mirkin G, Bognanni I, Holmberg J, Piazzón IM, Nepomnaschy I, Costa H, Cañones C, Raiden S, Vermeulen M, Geffner JR (2010) Mouse bone marrow-derived mesenchymal stromal cells turn activated macrophages into a regulatory-like profile. PLoS One 5:e9252. doi:10.1371/journal.pone.0009252

19. Malefyt RW, Abrams J, Bennett B, Figdor CG, de Vries JE (1991) Interleukin 10(IL-10) inhibits cytokine synthesis by human monocytes: an autoregulatory role of IL-10 produced by monocytes. J Exp Med 174:1209–1220

20. Manning E, Pham S, Li S, Vazquez-Padron RI, Mathew J, Ruiz P, Salgar SK (2010) Interleukin-10 delivery via mesenchymal stem cells: a novel gene therapy approach to prevent lung ischemia-reperfusion injury. Hum Gene Ther 21:713–727. doi:10.1089/hum.2009.147

21. Mantovani A, Sica A, Sozzani S, Allavena P, Vecchi A, Locati M (2004) The chemokine system in diverse forms of macrophage activation and polarization. Trends Immunol 25:677–686. doi:10.1016/j.it.2004.09.015

22. Marketou M, Kintsurashvili E, Papanicolaou KN, Lucero HA, Gavras I, Gavras H (2010) Cardioprotective effects of a selective B(2) receptor agonist of Bradykinin post-acute myocardial infarct. Am J Hypertens 23:562–568. doi:10.1038/ajh.2010.20

23. Nahrendorf M, Swirski FK, Aikawa E, Stangenberg L, Wurdinger T, Figueiredo JL, Libby P, Weissleder R, Pittet MJ (2007) The healing myocardium sequentially mobilizes two monocyte subsets with divergent and complementary functions. J Exp Med 204:3037–3047. doi:10.1084/jem.20070885

24. Oerlemans MI, Goumans MJ, van Middelaar B, Clevers H, Doevendans PA, Sluijter JP (2010) Active Wnt signaling in response to cardiac injury. Basic Res Cardiol 105:631–641. doi:10.1007/s00395-010-0100-9

25. Radin MJ, Holycross BJ, Dumitrescu C, Kelley R, Altschuld RA (2008) Leptin modulates the negative inotropic effect of interleukin-1beta in cardiac myocytes. Mol Cell Biochem 315:179–184. doi:10.1007/s11010-008-9805-6

26. Ritter M, Buechler C, Langmann T, Orso E, Klucken J, Schmitz G (2000) Regulation of scavenger receptor CD163 expression in human monocytes and macrophages by pro- and anti-inflammatory stimuli. J Leukoc Biol 67:97–103. doi:10.1159/000028105

27. Sanganalmath SK, Abdel-Latif A, Bolli R, Xuan YT, Dawn B (2011) Hematopoietic cytokines for cardiac repair: mobilization of bone marrow cells and beyond. Basic Res Cardiol 106:709–733. doi:10.1007/s00395-011-0183-y

28. Sarugaser R, Lickorish D, Baksh D, Hosseini MM, Davies JE (2005) Human umbilical cord perivascular (HUCPV) cells: a source of mesenchymal progenitors. Stem Cells 23:220–229. doi:10.1634/stemcells.2004-0166

29. Schuh A, Liehn EA, Sasse A, Schneider R, Neuss S, Weber C, Kelm M, Merx MW (2009) Improved left ventricular function after transplantation of microspheres and fibroblasts in a rat model of myocardial infarction. Basic Res Cardiol 104:403–411. doi:10.1007/s00395-008-0763-7

30. Stein M, Keshav S, Harris N, Gordon S (1992) Interleukin 4 potently enhances murine macrophage mannose receptor activity: a marker of alternative immunologic macrophage activation. J Exp Med 176:287–292

31. Stout RD, Jiang C, Matta B, Tietzel I, Watkins SK, Suttles J (2005) Macrophages sequentially change their functional phenotype in response to changes in microenvironmental influences. J Immunol 175:342–349

32. Tolar J, LeBlanc K, Keating A, Blazar BR (2010) Hitting the right spot with mesenchymal stromal cells (MSCs). Stem Cells 28:1446–1455. doi:10.1002/stem.459

33. Wu J, Li J, Zhang N, Zhang C (2011) Stem cell-based therapies in ischemic heart diseases: a focus on aspects of microcirculation and inflammation. Basic Res Cardiol 106:317–324. doi:10.1007/s00395-011-0168-x